

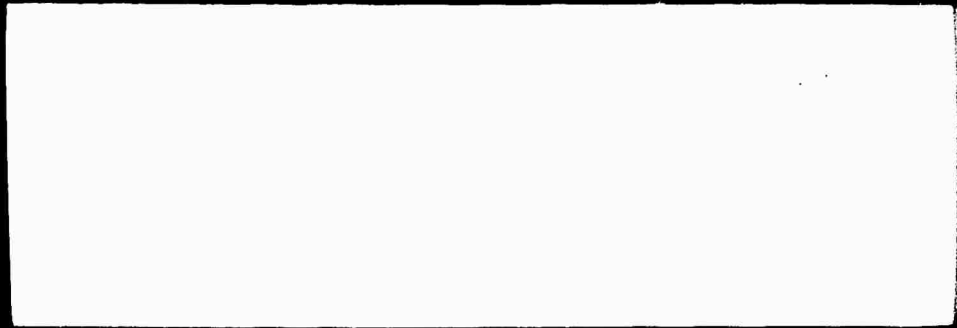
A REPORT FROM

OWENS-ILLINOIS TECHNICAL CENTER

710825



FORM NO. 60



(1)

CONSUMER & TECHNICAL PROJECTS DIVISION
RESEARCH, DEVELOPMENT & ENGINEERING

Reproduced by the
CLEARINGHOUSE
for Federal Scientific & Technical
Information Springfield Va. 22151

OWENS-ILLINOIS

(1)

DISCLAIMER NOTICE

THIS DOCUMENT IS THE BEST
QUALITY AVAILABLE.

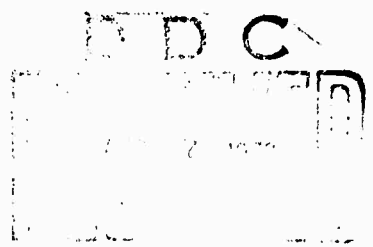
COPY FURNISHED CONTAINED
A SIGNIFICANT NUMBER OF
PAGES WHICH DO NOT
REPRODUCE LEGIBLY.

SPONSORED BY:
ADVANCED RESEARCH PROJECTS AGENCY
ARPA ORDER NO. 1441
PROGRAM CODE P9D10

SEMI-ANNUAL TECHNICAL REPORT
BY: ROBERT W. BECK

DAMAGE THRESHOLD STUDIES OF GLASS LASER MATERIALS

31 JULY 1970
CONTRACT NO. DAHC15-69-C-0303



CONTRACT DATE	30 JUNE 1969
CONTRACT EXPIRATION	30 JUNE 1971
CONTRACT AMOUNT	\$418,967

CONSUMER & TECHNICAL PRODUCTS DIVISION
OWENS-ILLINOIS, INC.
TOLEDO, OHIO
PHONE: (419) 242-6543, EXTENSION 33866

This document
is for public
distribution

FORWARD

The work outlined in this semi-annual report was performed under Contract DAHC15-69-C-0303, ARPA Order 1441, and Program Code P9D10. The work was performed within the Consumer and Technical Products Division of Owens-Illinois, Inc., Toledo, Ohio and covers the time period from 1 January 1970 through 30 June 1970.

The principal investigator for the program is R. W. Beck and the program manager is H. A. Lee. The thermodynamics of the melting of laser glass in platinum is being conducted by L. Spanoudis under the direction of P. R. Wengert. This contract is administered by the Chief, Defense Contract Administration Services Office, Toledo, Ohio. Dr. R. A. Huggins, Director for Materials Sciences, ARPA, is the Contracting Officer's Technical Representative.

TABLE OF CONTENTS

	<u>PAGE</u>
1. SUMMARY	1
2. ACTIVE DAMAGE TESTS	2
3. LIFE TESTS.	4
4. PASSIVE DAMAGE TESTS.	5
5. SELF-TRAPPING AND SURFACE DAMAGE TESTS.	6
6. APPLICATION OF THERMODYNAMICS TO LASER GLASS MELTING	13
6.1 Introduction	13
6.2 Discussion	14
6.3 Future Activities.	16
7. REFERENCES.	19

LIST OF FIGURES

- Figure 1 Self-Trapping and Surface Damage Experimental Arrangement
- Figure 2 Orange Peel Damage
- Figure 3 Orange Peel Damage
- Figure 4 Pitting Damage
- Figure 5 Pitting Damage
- Figure 6 Pitting Damage
- Figure 7 Trapping Damage
- Figure 8 Trapping Damage
- Figure 9 Trapping Damage

LIST OF TABLES

- Table 1 Active Damage Summary
- Table 2 Self-Trapping and Surface Damage Results
- Table 3 Potential Reactions in Glass Melt and Their
Standard Free Energies² at 1600°K
- Table 4 Systems Where the Activity Coefficients Have
Been Determined Based on the Solvent Standard
State
- Table 5 Compositions (Wt.%) of Some Commercially Avail-
able Laser Glasses

SUMMARY

The research goal of this program is to evaluate the radiation damage thresholds of neodymium doped glass laser materials and to determine the associated damage mechanism. The research objectives are to:

1. Determine the relationship between active and passive damage threshold evaluations.
2. Relate the damage thresholds to material homogeneity.
3. Evaluate damage threshold versus pulse duration.
4. Determine the kinetics of output degradation at 20, 30, and 50 joules/cm² average energy density.
5. Coordinate with and furnish samples to the Naval Research Laboratory (NRL) for comparative evaluations.
6. Coordinate with and furnish samples to the National Bureau of Standards (NBS) for damage mechanism studies.

The principal test facility for this study is a Q-switched, neodymium glass, laser oscillator-treble amplifier system developed by Owens-Illinois. A complete description of the facility may be found in Section 2 of the 31 January 1970, Semi-Annual Technical Report of the present contract.

During the work period 1 January 1970 through 30 June 1970 all phases of the research program were actively pursued except phase 3, which involves a determination of the relationship between internal inclusion type damage and pulse duration. This phase is being deferred to the succeeding 12 month extension of the present contract and the initial literature search of the thermodynamic analysis of the melting of laser glasses in platinum has replaced it during this reporting period.

A summary of the activities from 1 January 1970 through 30 June 1970 is as follows:

1. Twelve third amplifier rods, melted in platinum, were selected equally from each of two melts and actively tested to determine their inclusion type damage thresholds. The peak damage thresholds varied from 18.2 to 31.8 joules/cm² for the first melt and from 16.6 to 53.1

1. (continued)

- joules/cm² for the second melt. The average peak damage thresholds were 23.9 and 32.8 joules/cm² for the first and second melts respectively.
2. An 84% improvement in the inclusion type damage threshold of platinum melted laser glass has been realized in the time period from February 1969 to February 1970.
3. Active life tests in the third amplifier at average energy densities of 15 and 30 joules/cm² for 200 shot sequences indicate no system deterioration in efficiency, beam profile, beam divergence, or pulse duration, although in some cases as many as 10 to 12 inclusions were noted in the samples at the end of a test.
4. Passive damage measurements on samples approximately 0.5 cm thick by 2 cm square mapped at 100X magnification with side lighting, irradiated, and remapped, have proven unsuccessful in generating inclusion size and type versus damage threshold data. The difficulty arises from the small density of inclusions present in the material and from the fact that micron to sub-micron size inclusions appear to be the most easily damaged.
5. A passive test sample, which was visually inclusion free at 100X magnification with side lighting, subsequently showed no internal damage at a peak energy density of 70 joules/cm².
6. The literature search for the thermodynamic analysis of the melting of laser glass in platinum has been initiated. The activity coefficients for 13 binary systems have been found to date. No data has been found for ternary or higher order multicomponent oxide systems representative of current laser glasses.

2. ACTIVE DAMAGE TESTS

Active damage threshold measurements have been obtained for 12 additional third amplifier rods selected equally from each of two melts B and C. As for the previous measurements, damage was noted by the presence of a visible inclusion with the sample illuminated with a microscope lamp. This technique easily detects 10 μ size particles. At the onset of damage one or two damage sites were noted and they were generally in the order of from 100 μ to 200 μ in size. Table 1 summarizes the damage results for melts B and C. The

TABLE 1

ACTIVE DAMAGE SUMMARY

MELT "A" (February 1969)

SAMPLE NO.	AVERAGE DAMAGE THRESHOLD (Joules/cm ²)	PEAK DAMAGE THRESHOLD (Joules/cm ²)
1	8.0	17.8
2	10.5	17.3
3	12.0	19.2
4	6.5	10.9
5	9.8	15.7
6	23.9	31.1

Average = 11.9

Average = 17.8

MELT "B" (October 1969)

SAMPLE NO.	AVERAGE DAMAGE THRESHOLD (Joules/cm ²)	PEAK DAMAGE THRESHOLD (Joules/cm ²)
1	25.0	31.8
2	15.0	20.3
3	16.6	21.6
4	18.8	25.9
5	13.0	18.2
6	16.4	25.7

Average = 17.5

Average = 23.9

MELT "C" (February 1970)

SAMPLE NO.	AVERAGE DAMAGE THRESHOLD (Joules/cm ²)	PEAK DAMAGE THRESHOLD (Joules/cm ²)
1	41.6	52.6
2	13.8	16.6
3	19.4	23.1
4	26.1	33.1
5	46.9	53.1
6	13.8	18.6

Average = 26.9

Average = 32.8

previously reported damage results, melt A, are included for reference. The table indicates both the average and the peak damage thresholds for each rod tested. As shown, the highest damage thresholds obtained to date have been samples one and five of melt C which damaged at peak energy densities of 52.6 and 53.1 joules/cm² respectively. It is significant to note that the range of damage thresholds within a melt is of the same order as the melt average, indicating that the damage sites are not uniformly distributed throughout the melt either in size, location, or both. An analysis of the data also shows that the average of the peak damage thresholds for melt C is 84% greater than the corresponding figure for melt A, indicating a significant improvement in melting capabilities in the time period from February 1969 to February 1970.

It is anticipated that when the thermodynamic analysis of the melting environment is completed, the results will dictate further improvements in the coming months.

3. LIFE TESTS

In the active damage threshold measurements which have just been discussed, laser glass damage is defined as the occurrence of an inhomogeneous physical defect within the material resulting from the transmission of a laser pulse. Although this is certainly a meaningful definition, the users of laser glass materials are more interested in a measure of system performance. An alternative definition of laser glass damage, then, is a degradation in the output performance of the laser system in terms of some system variables, such as efficiency, beam profile, beam divergence, or pulse duration.

To determine the significance of such a proposed degradation definition of laser glass damage, rods were actively life tested in the third amplifier

The results of the present study are listed in Table II under energy density. Initial attempts to determine the laser penetration range and field of view were made at the time of the first test. The size of an aperture on the laser output lens was varied to give a wide range of spot sizes and beam profiles. The results were generally similar, but the laser efficiency was not constant. Each 100 shot sequence was repeated with a system deterioration in efficiency, beam profile, and divergence, as well as a small, although not critical, laser glass damage. The results of the samples at the end of the tests. These results imply that for the present state-of-the-art of laser tubes, system degradation due to laser glass damage is not a major concern.

3. PASSIVE DAMAGE TESTS

At the outset of the current laser glass damage program one of the primary goals was to generate inclusion size and type versus damage threshold data. To attain this goal, samples approximately 0.5 cm thick by 2 cm square were polished and mapped at 100X magnification with side lighting. The samples were then irradiated and remapped.

After evaluating many such samples, it must be concluded that such a technique is not practical. First, due to small density of potential damage sites within the material, the samples must be mapped to locate the desired inhomogeneities. Second, when inhomogeneities are located they rarely damage when irradiated, rather, small micron to sub-micron size defects, which show up with the side lighting, produce the majority of the damage and wash out the original sites. Third, quite often damage occurs in areas where the glass was thought to be inclusion free. Attempts are presently being made to locate the defects with holographic techniques but, if the lowest damaging inclusions

are in fact those of a micron to sub-micron size, then even holography may not have the necessary resolving power.

One passive damage measurement worth noting is a sample which was visually inclusion-free at 100X magnification prior to irradiation and subsequently showed no damage at a peak energy density of 70 joules/cm². If this sample is indeed inclusion free then, the damage threshold of homogeneous glass is quite high.

5. SELF-TRAPPING AND SURFACE DAMAGE TESTS

Preliminary self-trapping and surface damage measurements have been performed on a 91 cm long unpumped sample. The sample was first irradiated with the unfocused output of the oscillator-amplifier system and neither surface or self-trapping damage occurred for a maximum average energy density of 73 joules/cm² incident on the front surface of the sample. Assuming a beam divergence of 2 milli-radians, this is equivalent to an energy density of 63 joules/cm² on the output surface of the sample.

Having produced no damage with the unfocused beam, a 2 meter lens was placed in the system as shown in Figure 1. With this arrangement, as the output energy of the laser was increased the first appearance of damage was an orange peel effect on the output surface of the test sample. Examples of this type of damage may be found in Figures 2 and 3. In Figure 2 the surface is slightly out of focus to more effectively show the waviness, while in Figure 3 the surface is in focus and both the orange peel and pitting damage are apparent. Sampling the output surface at several locations showed that this type of damage occurs on the average at an energy density of 136 joules/cm².

As the output energy was further increased, pitting damage began to appear on the output face. The onset of such damage on the average occurred

SELF-TRAPPING & SURFACE DAMAGE EXPERIMENTAL ARRANGEMENT

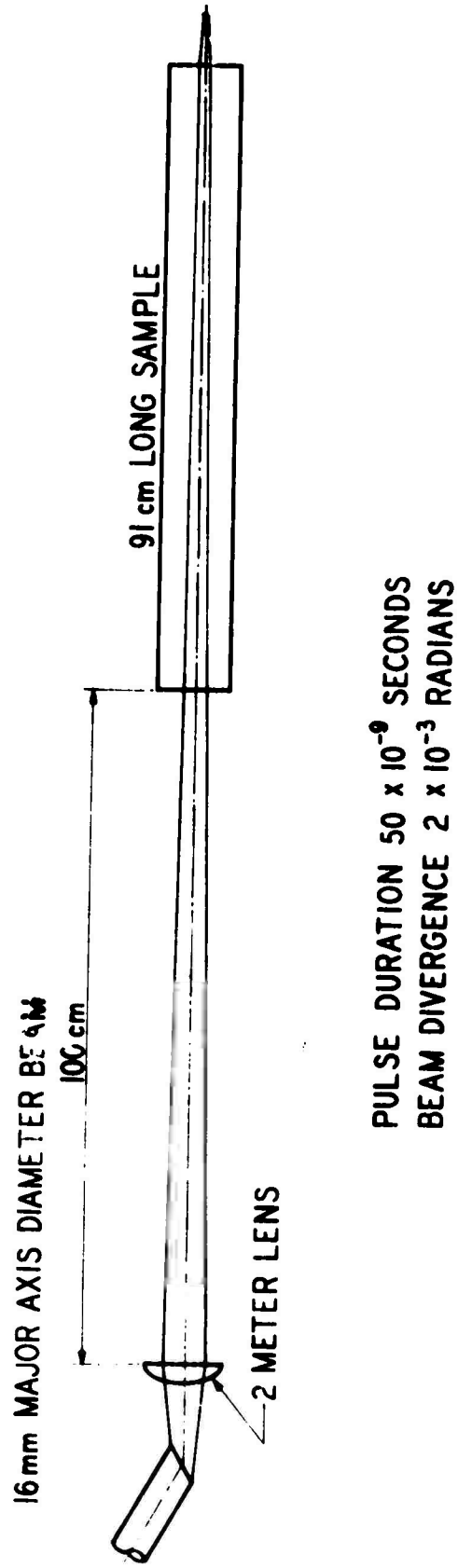


FIGURE 1

ORANGE PEEL DAMAGE

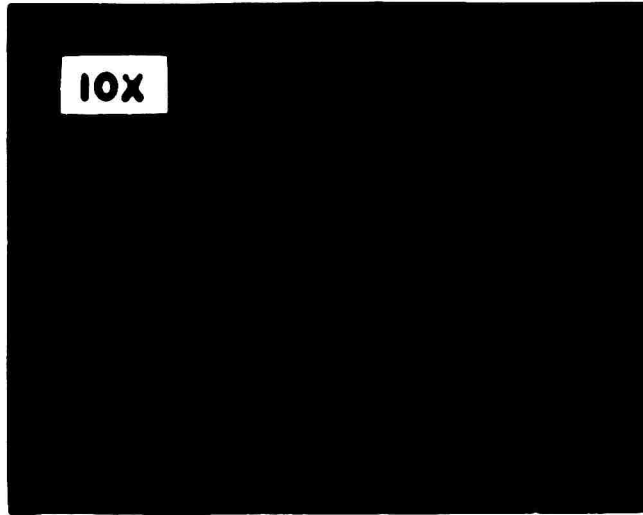


FIGURE 2

ORANGE PEEL DAMAGE



FIGURE 3

NOT REPRODUCIBLE

at an energy density of 144 joules/cm^2 , somewhat above the level for the crater type damage. The appearance of this type of damage at threshold was generally marked by the presence of crater type damage surrounded by a larger region of crater rim. Several such situations are shown in Figures 4, 5, and 6 as the damage progresses from threshold to several times threshold. No front surface damage was noted during these tests for a maximum average energy density of 140 joules/cm^2 .

Throughout the surface damage testing, self-trapping damage was noted. The trapping damage occurred anywhere from the front end to the exit end of the filament and generally occurred only after exit surface damage was noted, such that the exit face damage does not appear to be trapping limited. The average trapping threshold was found to be 128 joules/cm^2 . Figures 7, 8, and 9 are typical of the trapping damage noted. As shown, the bubble type damage characteristically has a diameter of a few tens of microns and the spacing between bubbles is generally not uniform. A summary of the self-trapping and surface damage results is shown in Table 2. The table primarily indicates the rather broad variation in the damage results, especially those related to the trapping threshold which varied from 63 to 194 joules/cm^2 . Because of these rather large variations, this data should be considered as tentative only. Further tests are presently being prepared and in the near future the range for the damage threshold values will hopefully be narrowed. It cannot be ignored, however, that these damage levels are generally higher than those previously reported by others.

PITTING DAMAGE



FIGURE 4

PITTING DAMAGE

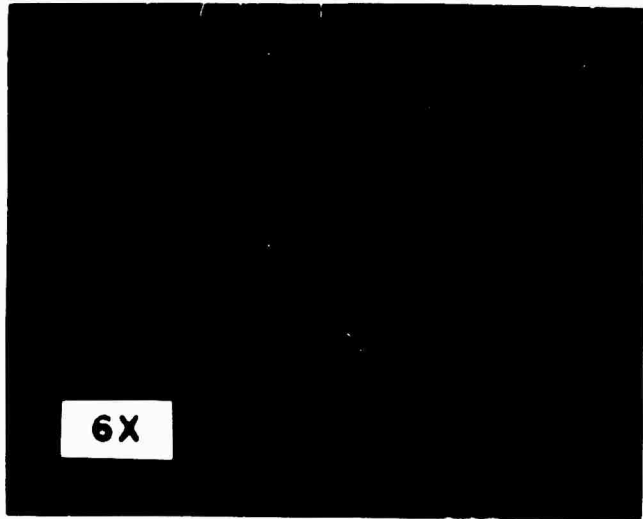


FIGURE 5

PITTING DAMAGE

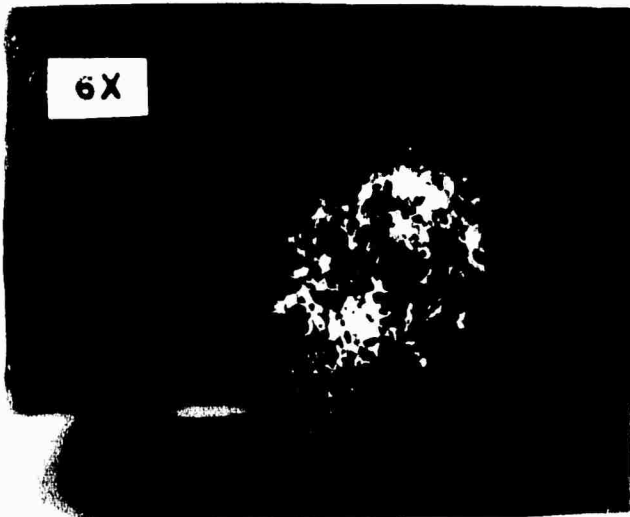


FIGURE 6

NOT REPRODUCIBLE

TRAPPING DAMAGE

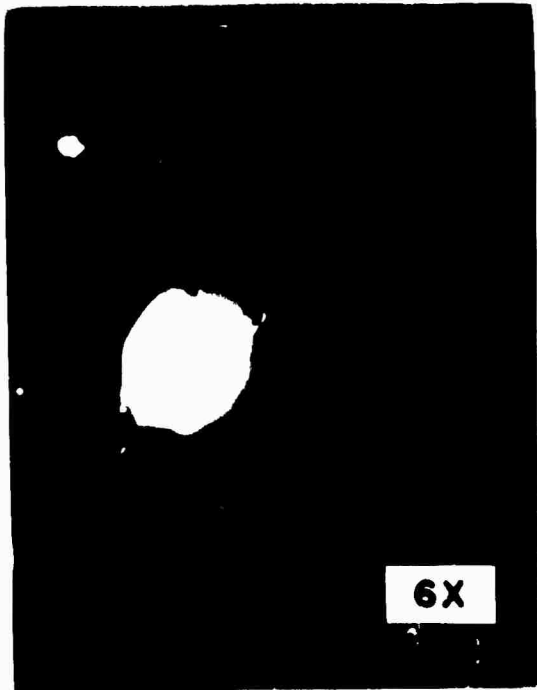


FIGURE 7

TRAPPING DAMAGE

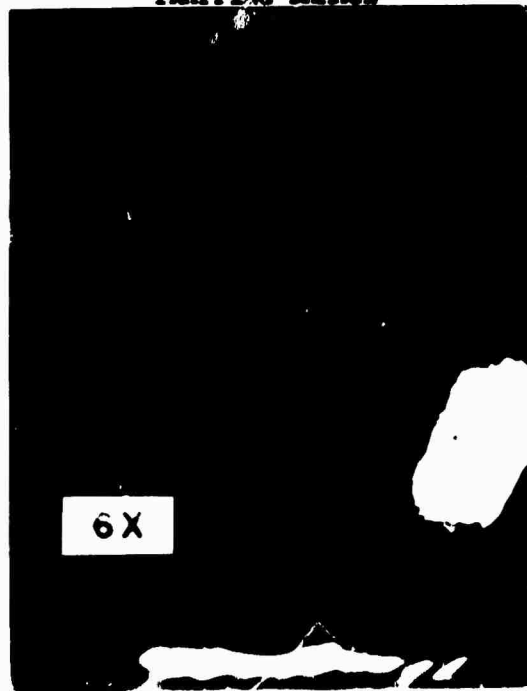


FIGURE 8

TRAPPING DAMAGE

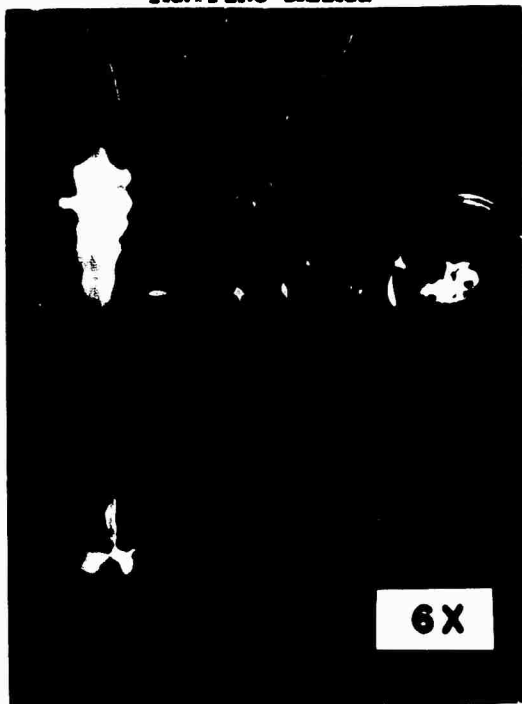


FIGURE 9

NOT REPRODUCIBLE

TABLE 2

SELF-TRAPPING &
SURFACE DAMAGE RESULTS

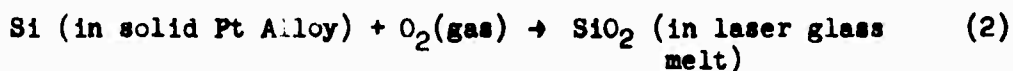
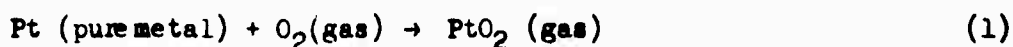
ORANGE PEEL (Average Joules/cm ²)	SURFACE PITTING (Average Joules/cm ²)	TRAPPING (Average Joules/cm ²)
134	123	83
171	154	63
112	150	170
113	150	194
147		

6. APPLICATION OF THERMODYNAMICS TO LASER GLASS MELTING

6.1 Introduction

Pt inclusions in laser glass appear to be caused by the migration of Pt as the platinum oxide gas, PtO_2 , and the subsequent reprecipitation of Pt. Thermodynamics is being applied to the melting procedure in order to reduce the partial pressure of PtO_2 , thereby reducing the number of inclusions.

The Pt metal can be stabilized with respect to its oxide by reducing the partial pressure of $O_2(P_{O_2})$. In stabilizing the Pt metal, the oxides in the glass melt are destabilized in favor of their metals resulting in the formation of Pt alloys. The following reactions illustrate this problem.



As the P_{O_2} is reduced both Si and Pt are stabilized with respect to their oxides. It is apparent that the P_{O_2} must be chosen so that the P_{PtO_2} is as low as possible without the laser melt oxides being reduced to the metal and attacking the Pt crucible.

In order to choose the appropriate P_{O_2} , the following information is required:

(1) the standard state free energy of Reaction (1); (2) the standard state free energy for the reactions similar to Reaction (2) for all oxides in the laser glasses; (3) the activities of the various oxides in laser glasses; and (4) the activities of the corresponding metals in Pt. From the relationship between the activity of the i th component (a_i), the mole fraction (x_i), and the activity coefficient (γ_i'):

$a_i = x_i \gamma_i$; it can be seen that the activity coefficients of the various components (γ_i) may also be used.

The standard state free energy of Reaction (1) has been determined by Alcock and Hooper:¹

$$\Delta F^\circ = \Delta F^\circ_f(\text{PtO}_2) = 39.270 + 340 - T(0.93 + 0.21) \text{ cal/mole of PtO}_2$$

The standard state free energies for the formation of the common oxides in glass have been determined² and are presented in Table 3. The ΔF° 's correspond to the energy difference between reactants and products when the solids and liquids are pure and when the gases are at 1 atmosphere pressure. The activities yet to be determined take into account the fact that the oxides are in a glass solution and that the metals are in a Pt alloy. Rather than reporting the activity of a species in the literature, the activity coefficient is the preferred variable.

The goal of this program, therefore, is to determine the γ_i 's of oxides in laser glass and the γ_i 's of the metals of the laser glass oxides in Pt.

6.2 Discussion

A literature search has been initiated. A preliminary review showed that thirty-five authors have done work in the area; they were contacted for any additional information. Nine authors have responded to date; their replies indicate that the preliminary search was rather complete.

Nine government agencies and twelve private agencies have been contacted. Searches are currently underway by Science Information Exchange, NASA, and Aerospace Research Applications Center.

TABLE 5
 POTENTIAL REACTIONS IN GLASS MELT
 AND THEIR STANDARD FREE ENERGIES² AT 1600°C

	ΔF° (kcal/mole O_2)
2 $CaO(s) \rightarrow 2 Ca(l) + O_2$	16.2
4 $Ce_2O_3(s) \rightarrow 4 Ce(l) + O_2$	34.2
2 $Fe_2O_3(s) \rightarrow 4 Fe(l) + O_2$	44.6
2 $Hf_2O_3(s) \rightarrow 4 Hf(l) + O_2$	65.3
2 $FeO(s) \rightarrow 2 Fe(l) + O_2$	77.2
$SiO_2(s) \rightarrow Si(l) + O_2$	142.0
2 $SiO_2(s) \rightarrow 2 SiO(g) + O_2$	176.0
2 $U_2O_3(s) \rightarrow 4 U(l) + O_2$	176.8
2/3 $Al_2O_3(s) \rightarrow 4/3 Al(l) + O_2$	185.2
2/3 $Er_2O_3(s) \rightarrow 4/3 Er(l) + O_2$	205.8
2/3 $Ce_2O_3(s) \rightarrow 4/3 Ce(l) + O_2$	205.8
2 $CaO(s) \rightarrow 2 Ca(l) + O_2$	221.4
2 $Al_2O_3(s) \rightarrow 4 AlO(g) + O_2$	483.2

6.2 (continued)

A search through Chemical Abstracts uncovered no thermodynamic information in addition to the data already obtained.

Table 4 indicates the binary systems for which the activity coefficients have been found to date.

No data has been found for ternary or higher order multicomponent oxide systems representative of the complex laser compositions currently used as listed in Table 5.^{13, 14} Once the literature search has been completed, estimates of activities in the multicomponent systems will be made based upon the data from binary systems.

6.3 Future Activities

The program includes the experimental measurement of activities in a laser glass as well as the completion of the literature review. The best estimate of activity coefficients will aid the planned experimental work.

TABLE 9

SOLUBILITY DATA FOR AMMONIUM COMPOUNDS HAVE BEEN
 EXCLUDED AND LISTED IN THE INVERSE STANDARD STATE

<u>System</u>	<u>References</u>
Al-H ₂ O	3
Bi-H ₂ O	3
Bz-H ₂ O	1,7,10,11
Ca-H ₂ O	6,7
Cl-H ₂ O	7
Mn-H ₂ O	7
Li ₂ S-SiO ₂	4,9
La ₂ O-SiO ₂	4,9
N ₂ O-SiO ₂	4,9
CaO-SiO ₂	8,9
MgO-SiO ₂	9
BaO-SiO ₂	9
MnO-SiO ₂	9
SnO-SiO ₂	9
As ₂ O-SiO ₂	9
Ni ₂ O-SiO ₂	9
W ₂ O-SiO ₂	9
SiO ₂ -TiO ₂ -B ₂ O ₃ -Al ₂ O ₃	12

TABLE 5
COMPOSITIONS (WT.%) OF SOME COMMERCIALLY
AVAILABLE LASER GLASSES

Oxide	GLASS NO.							
	1	2	3	4	5	6	7	8
SiO ₂	67	62	68	31	63	67	72	59
TiO ₂	-	-	0.5	-	-	-	-	-
B ₂ O ₃	-	-	-	13	-	-	-	-
Al ₂ O ₃	-	2	-	8	6	1	1.5	-
Sb ₂ O ₃	-	1	2	-	-	1	-	1.0
As ₂ O ₃	-	-	-	1	-	-	-	-
CaO	-	-	-	-	11	-	-	-
BaO	3	3	4	42	-	5	5.0	22.0
PbO	-	-	1.5	-	-	-	-	-
ZnO	-	2	-	-	-	2	1.3	-
Li ₂ O	-	1	-	-	15	1	1.0	-
Na ₂ O	7	6	4	-	-	7	7.5	-
K ₂ O	15	18	17	-	-	11	7.5	12.0
Nd ₂ O ₃	5	5	3	5	5	5	4.2*	6.0*
Misc.	3	-	-	1	-	-	-	-

* Nd₂O₃ was used or similar dopant, such as Er₂O₃. Glasses 1-6 are from reference No. 13, Glasses 7 and 8 are from reference 14.

REFERENCES

1. C. E. Alcock and G. W. Hooper, "Thermodynamics of the Gaseous Oxides of the Platinum-Group Metals", Royal Society Proc. 254, 951-961, 1960.
2. Bulletin 542, U. S. Bureau of Mines, 1959.
3. P. J. Hawles, et al., Journal of the Iron and Steel Institute, Feb., 1964, 113-121.
4. R. J. Charles, Journal of the American Ceramics Society, Vol. 50, No. 12 1967, 631-641.
5. H. R. Larsen and J. Chipman, Acta Metallurgica, Vol. 2, Jan., 1954, 1-2.
6. K. Schwerdtfeger and A. Muan, Acta Metallurgica, Vol. 12, Aug. 1964, 905-909.
7. A. Muan, Thermodynamics, Vol. II, International Atomic Energy Agency, Vienna, 1966.
8. R. J. Charles, Physics and Chemistry of Glasses, Vol. 10, No. 5, Oct. 1969, 169-178.
9. M. Rey, Discussions of the Faraday Soc. 4, 1968, 257-265.
10. E. F. Heald, Transactions of the Metallurgical Society of AIME, Vol. 239, Sept., 1967, 1337-1340.
11. R. W. Taylor and A. Muan, Transactions of the Metallurgical Society of AIME, Vol. 224, June, 1962, 500-502.
12. H. Rein and J. Chipman, Transactions of the Metallurgical Society of AIME, Vol. 223, Feb., 1965, 415-425.
13. Emil W. Deeg, "Toughening a 'Glass Jaw' ", Laser Focus, 38-39, March, 1969.
14. John F. Kreidl, "The History of the Glass Laser", The Glass Industry, 535-537, October, 1967.